Synthesizing Axial Inserting p−n Heterojunction Nanowire Arrays for Realizing Synergistic Performance

Haowei Lin, Huibiao Liu,* Xuemin Qian, Songhua Chen, Yongjun Li, and Yuliang Li*

CAS Key Laboratory of Organic Solids, Beijing National Laboratory for Molecular Sciences (BNLMS), Institute of Chemistry, Chinese Academy of Sciences, Beijing 100190, P. R. China

Ⓢ *Supporting Information*

ABSTRACT: Consideration of the material design and components match on structure and energy, the solid−solid combined nanowires of p-type conductive polymer of poly[3-thiophene carboxylic acid methyl ester] (PTCM) and n-type inorganic semiconductor PbS was prepared with a 2.57 μm^2 heterojunction interface. The axial deeply inserting heterojunction nanowire arrays exhibited excellent rectifying features and diode nature, as well as obvious electrical switching behavior, which are much excelled individual components of PTCM and PbS nanowire arrays for realizing synergistic performance.
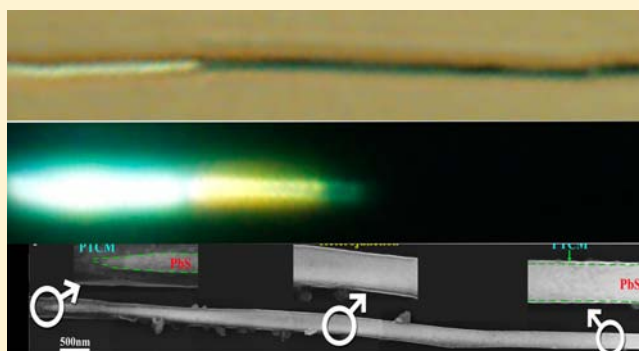
INTRODUCTION

One-dimensional p−n heterojunction nanostructures and materials have recently attracted considerable attention due to their unique optical, optoelectronic, and electronic properties.[1−14] Recently, researchers have developed an approach for synthesizing and characterizing many new structures and materials with different shapes, dimensions, and morphologies.[15−18] In general, the heterojunction materials are focused to three categories: (i) inorganic/inorganic, (ii) inorganic/organic, and (iii) organic/organic,[19−33] and expected to be widely applied in interdisciplinary research of molecular electronics. Among these structures, one-dimensional p−n inorganic/organic heterojunction nanowires have been demonstrated to incorporate a wide range of elemental and material compositions, including organics, inorganics, and hybrid structures, and have exhibited excellent photovoltaic, rectification, and light-emitting behavior.[34−40] The solid−solid combination of inorganic and organic components to form functionalized surfaces and interface has been a key factor of synergistic performance.[41] The larger interface of the heterojunction is in favor of transfer, transport, and separation of electron and charge, which is very important in the bulk heterojunctional photovoltaic devices. It is significant in material chemistry to create new heterojunctions on the interface of aggregate structures that combine the optical and electrical properties of organic semiconductor with the high stability of inorganic semiconductors. Therefore, how to combine two or three individual components and control their growth of one-dimensional structure with a solid−solid ordered interface is a significant and ongoing challenge in the materials field.

Recently, some researchers have focused on preparation and self-assembly of p−n junctions with electrical and photoelectrical properties on the nanoscale.[29] However, there has been no report in fabrication of heterojuction structures with a larger interface linking between two components. We prepared novel p−n axial inserting heterojunction nanowire arrays of poly[3-thiophene carboxylic acid methyl ester] (PTCM)/PbS which show a very unique interface structure with a larger size interface by inserting an organic moiety into an inorganic component. The inserting axial p−n heterojunction exhibited excellent rectifying features and a diode nature, as well as an obvious electrical switching behavior which are much excelled as compared with that of individual PTCM and PbS nanowire arrays for realizing synergistic performance, due to the big linking interface interaction by inorganic and organic.

EXPERIMENTAL DETAILS

Materials. All chemicals were purchased from Aldrich Corporation and Beijing Chemical Reagent Corporation, China. All of the reagents were used as received. The anodic aluminum oxide (AAO) templates with a porous diameter of 200 nm, a thickness of 60 μm, and a diameter of 1.3 mm were purchased from Whatman Co. The nanowires were synthesized by a homemade electrical cell with a diameter of 4 mm.

Synthesis of Poly[3-thiophene carboxylic acid methyl ester] (PTCM)/PbS Heterojunction Nanowire Arrays. 3-Thiophenecarboxylic acid (2.0 g, 15.6 mmol) was dissolved in MeOH (27 mL), and 18.4 M sulfuric acid (1.5 mL) was added. The reaction mixture was refluxed for 4 h, and then concentrated under reduced pressure. A saturated $NaHCO_3$ aqueous solution was added, and the mixture was extracted with ethyl acetate. The organic phase was dried over Na_2SO_4

and concentrated in a vacuum to give 1.98 g (14 mmol) of 3-thiophene carboxylic acid methyl ester as a colorless liquid.

PTCM/PbS heterojunction nanowire arrays were synthesized within the pores of anodized aluminum oxide (AAO) templates using electrochemical deposition technology (EDT) (Scheme 1). The

Scheme 1. Model of a Single PTCM/PbS Heterojunction Nanowire in a Pore of AAO Template
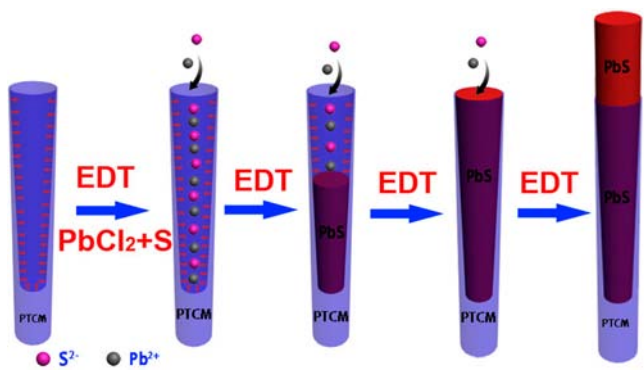
electrodeposition of PTCM was carried out in a three-electrode electrochemical cell with a diameter of 4 mm. Before electrochemical deposition, a layer of gold with 100 nm thickness was sputtered on one side of the AAO template via an ion sputtering system to serve as a working electrode. A piece of platinum plate and a saturated calomel electrode (SCE) were used as the counter and reference electrodes, respectively. The PTCM deposition was carried out from a 0.1 M boron trifluoride diethyl etherate (BFEE) solution of 3-thiophene carboxylic acid methyl ester by applying a voltage of 1.75 V (vs SCE) for an appropriate time (typically 5400 s). After deposition, the as-prepared samples were taken out from the electrolyte, rinsed several times with acetone, and then dried in air at room temperature. In the following electrodeposition process of PbS, the AAO template containing PTCM nanowires was used as the working electrode, and a platinum wire was used as the counter electrode. PbS nanowires were deposited into the AAO template at a current density of 2.5 mA/cm^2 in a DMSO solution consisting of 28 mM PbCl$_2$ and 95 mM element sulfur at 115 °C for 5400 s. Finally, the PTCM/PbS heterojunction nanowires embedded in an AAO membrane were prepared after the template was washed with hot DMSO and acetone several times, respectively. The AAO template with nanowires was selectively etched by NaOH aqueous solution (2 M) and cleaned by deionized water for later characterization.

Synthesis of PTCM and PbS nanowire arrays. The electrolyte used for PTCM nanowire electrodeposition was composed of a 0.1 M BFEE solution of 3-thiophene carboxylic acid methyl ester. A piece of platinum plate and a saturated calomel electrode (SCE) were used as the counter and reference electrodes, respectively. PTCM nanowires were deposited at 1.75 V, and the electrodeposition was kept running for 5400 s. After deposition, the AAO template was rinsed several times with acetone. PbS nanowires were deposited into the AAO template at a current density of 2.4 mA/cm^2 in a DMSO solution consisting of 28 mM PbCl$_2$ and 95 mM sulfur at 115 °C. Then, the AAO template was washed with hot DMSO and acetone several times, respectively.

Preparation of the Devices Based on PTCM/PbS Heterojunction, PTCM and PbS Nanowire Arrays for Electrical Property. The template was first removed partly by NaOH aqueous solution (2 M) to bulge the PbS nanowires, cleaned by deionized water and acetone, and then dried in air at room temperature. The PTCM/PbS heterojunction nanowire array film (the contacted area of the film was about 10 mm^2) was put on an ITO sheet, the PTCM side with Au film of that contacted the ITO sheet as cathode, then covered with a round aluminum foil with a diameter of 1.78 mm on top of the film (bulged PbS nanowire) as an anode. To ensure the separation between aluminum foil and ITO in the experiment, all the devices measured in our experiment were made in a top-contact device configuration.[40] The construction of PTCM and PbS nanowire array devices was the same as the PTCM/PbS heterojunction nanowire array device.

Characterization. Field emission scanning electron microscopy (SEM) and energy-dispersive X-microanalysis spectrum (EDS) patterns were taken with a JEOL JSM 4800F FESEM microscope at an accelerating voltage of 15 kV. The transmission electron microscopy (TEM) and high resolution transmission electron microscopy (HRTEM) measurements and selective-area electron diffraction patterns (SAED) were taken with a JEOL 2011 transmission electron microscope at an accelerating voltage of 200 kV. Confocal laser scanning microscopy (CLSM) images were acquired with a WITec CMR200 in the confocal Raman spectra mode. Current−voltage (I−V) characteristics of devices were recorded with a Keithley 4200 SCS at room temperature in air.

The electrochemical measurement of the PTCM film was performed in an electrolyte consisting of a 0.1 mol/L tetrabutylammonium hexafluorophosphate (TBAPF$_6$) acetonitrile solution. The PTCM film on an ITO substrate was used as the working electrode, and a platinum wire and a saturated calomel electrode (SCE) were used as the counter and reference electrodes, respectively. In this work, $E_{LUMO} = -e(\varphi_n' + 4.4)$, $E_{HOMO} = -e(\varphi_p' + 4.4)$, where E_{LUMO} is the LUMO energy level, E_{HOMO} is the HOMO energy level, and all
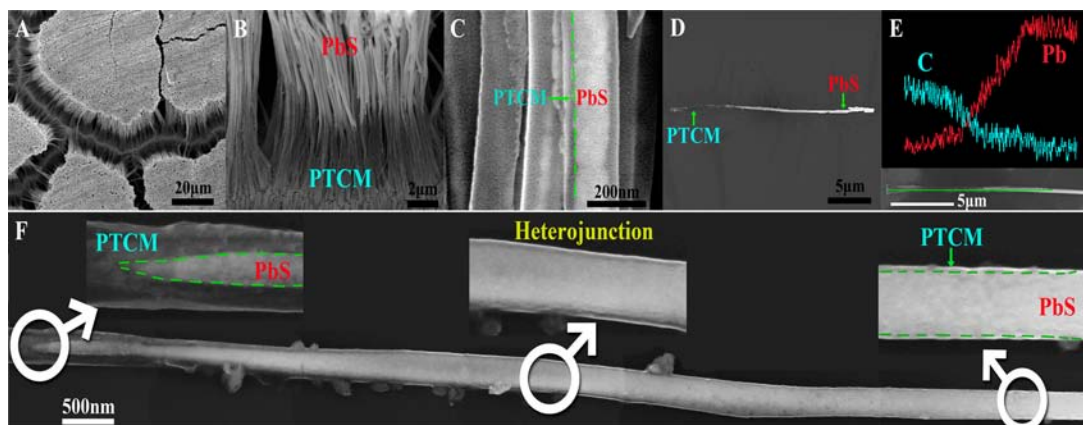
Figure 1. SEM images of PTCM/PbS heterojunction nanowires: (A) top view under a low magnification; (B) cross view; (C) the p−n junctions of PTCM/PbS heterojunction nanowires under a large magnification; (D) a typical single PTCM/PbS heterojunction nanowire; (E) element mapping of linear scanning of a single PTCM/PbS heterojunction nanowire; (F) the p−n heterojunction of a single PTCM/PbS nanowire (the insets are the different positions of the p−n heterojunction under a large magnification).

electrode potential values are vs SCE as the reference electrode. The onset potentials φ_p' and φ_n' were determined from the intersection of the two tangents drawn at the rising oxidation and reduction current and background current in the cyclic voltammograms.[42] To the PTCM film (see Figure S1A, Supporting Information), $E_{LUMO} = -3.2$ eV and $E_{HOMO} = -5.7$ eV.

■ RESULTS AND DISCUSSION

We designed and synthesized the p-type organic semiconductor of poly[3-thiophene carboxylic acid methyl ester] (PTCM) and used the n-type inorganic semiconductor of PbS to prepare axial deeply inserting heterojunction nanowire arrays by an associated approach. The model of PTCM/PbS heterojunction nanowire arrays prepared by the combination process was shown in Scheme 1. The p-type conductive polymer of PTCM with good conductivity can strongly combine with the n-type inorganic semiconductor PbS by coordination of interactions between carbonyls of PTCM and Pb^{2+} ions of PbS. The morphologies and size of the PTCM/PbS heterojunction nanowire arrays are characterized by SEM. Figure 1A revealed PTCM/PbS heterojunction nanowire arrays. As shown in Figure 1B, the nanowires with a smooth surface were well-defined with a diameter of about 200 nm and a length of about 60 μm. The dark part is PTCM with a length of about 4 μm, and the bright part is PbS with a length of about 45 μm. Some typical heterojunction nanowires of PTCM/PbS were shown in Figure 1C, and the clear interface between organic and inorganic semiconductors could be observed. The outer layer transparent part of the heterojunction nanowire was PTCM, and the inner layer dark part was PbS. This heterojunction nanowire formed a novel axial inserting structure, which was completely different from the axial heterojunction nanowires. Figure 1D showed a typical single PTCM/PbS heterojunction nanowire. The p−n heterojunction of the single PTCM/PbS heterojunction was displayed in Figure 1F. As shown in SEM and TEM images, the section of the heterojunction in the PTCM/PbS p−n heterojunction nanowire is approximatively conical. Thus, the area of the interface of the PTCM/PbS heterojunction nanowire could be calculated from the equation $S = \pi R(L^2 + R^2)^{1/2}$, where R, L, and S are the radius (i.e., 100 nm), length, and area of the heterojunction interface of the PTCM/PbS nanowire, respectively. The length of the p−n heterojunction is up to 8.2 μm, and the area of the heterojunction interface is 2.57 μm^2, which is 82 times the area of the end-to-end axial heterojunction interface. The insets of Figure 1F displayed three typical positions of inserting heterojunctions. At the starting end of the heterojunction nanowire was PTCM nanowire (the left panel of the insets); then, the PbS nanowire began to grow and wrapped inside the PTCM (the middle panel of the insets). The PTCM layer gradually thinned, and PbS gradually grew and finally formed integrated PbS nanowire (from left to right in Figure 1F). We directly demonstrated the embedded structure of an as-prepared nanowire by linear scanning (Figure 1E) in SEM, which showed the dispersion of C and Pb elements. In the two ends of the nanowire, the content of C and Pb elements remained stable. In the middle of the nanowire, with the gradual reduction of C element content, Pb element content gradually increased, which indicated that PTCM and PbS wrapped each other in the heterojunction and the hetero-junction was an axial inserting structure. The EDS patterns (Figure S4B, Supporting Information) confirmed that the heterojunction nanowire was composed of PTCM and PbS.

The axial inserting structure of the PTCM/PbS p−n heterojunction nanowire can also be confirmed by CLSM (Figure 2). Figure 2A presents some PTCM/PbS hetero-
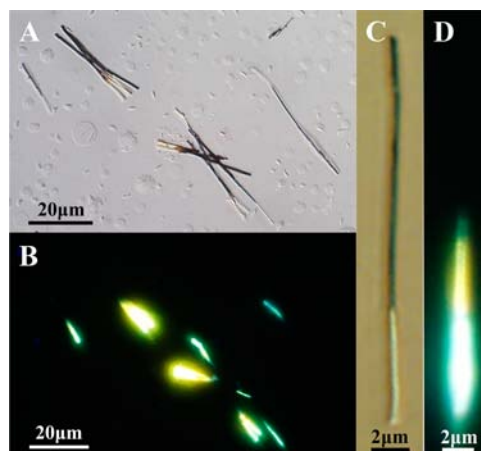
Figure 2. CLSM images of PTCM/PbS heterojunction nanowires: (A) optional image of PTCM/PbS heterojunction nanowires; (B) fluorescent image of PTCM/PbS heterojunction nanowires under the excitation of 330−380 nm; (C) optional image of a single PTCM/PbS heterojunction nanowire; (D) fluorescent image of a single PTCM/PbS heterojunction nanowire under excitation of 330−380 nm.

junction nanowires with a length of about 60 μm, the pale yellow end of which is PTCM and the black end is PbS. The corresponding fluorescent images of these nanowires in Figure 2B reveal the different parts of the heterojunction nanowire exhibited different fluorescence under the excitation of 330−380 nm. Parts C and D of Figure 2 show the optical and fluorescent images of a typical single PTCM/PbS hetero-junction nanowire under the excitation of 330−380 nm, respectively. In Figure 2D, the part with cyan fluorescence in the single PTCM/PbS nanowire is the PTCM segment. The yellow part corresponds to the PTCM/PbS heterojunction part, and PbS does not exhibit any fluorescence. In the PTCM/PbS heterojunction part, due to the fluorescence quenching effect of PbS to PTCM, fluorescence gradually weakened until quenching with the increase of PbS content, which clearly displays the axial inserting heterojunction structure and the interface length of about 8 μm of the PTCM/PbS nanowire.

TEM and HRTEM characterizations of the PTCM/PbS p−n heterojunction nanowires exhibited more structure information, as shown in Figure 3. Figure 3A displayed some typical PTCM/PbS heterojunction nanowires with a smooth surface and length of about 60 μm. A typical single PTCM/PbS heterojunction nanowire with a diameter of about 200 nm was shown in Figure 3B. Figure 3E displayed the p−n heterojunction with inserting structure of an independent PTCM/PbS nanowire under a higher magnification, which agrees well with the SEM image. The heterojunction interface formed by PbS and PTCM could be clearly observed according to the different brightness of the nanowire in the insets of Figure 3E. The heterojunction is a typical core−shell structure. The outer bright part was PTCM shell and gradually thinned, and the inner dark part was PbS core, which gradually changed thick with increase of length. The length of the heterojunction was 7.9 μm, and the interface between the inorganic and organic components was very solid. The SAED of different
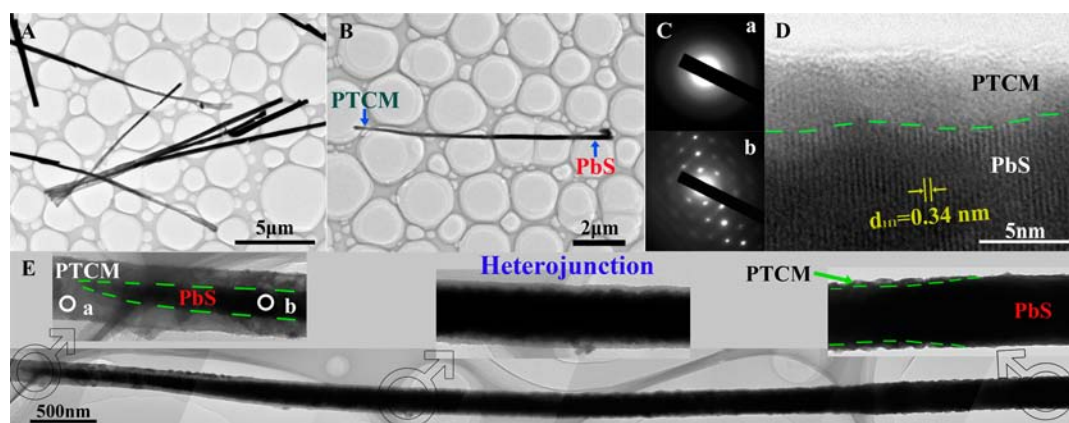
Figure 3. TEM images of PTCM/PbS heterojunction nanowires: (A) PTCM/PbS heterojunction nanowires; (B) a typical single PTCM/PbS heterojunction nanowire; (C) SAED patterns taken from segments in the single PTCM/PbS heterojunction nanowire, (a) PTCM part and (b) PbS part; (D) HRTEM image of the heterojunction interface of PTCM/PbS nanowire; (E) the p−n heterojunction of a single PTCM/PbS nanowire (the insets are the different positions of the p−n heterojunction under a higher magnification).
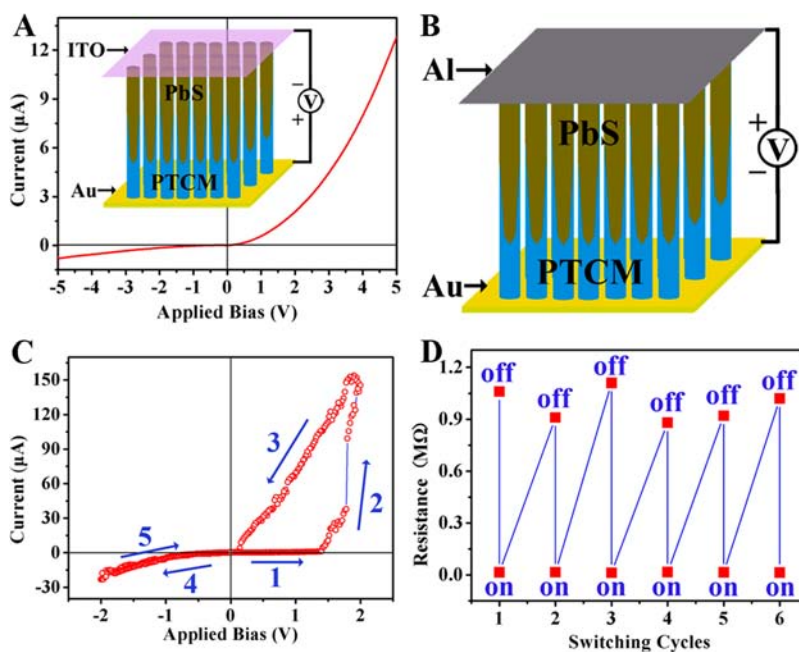
Figure 4. (A) Typical I−V curve of PTCM/PbS heterojunction nanowire arrays (the inset is its working model); (B) working model of the Al/PbS/PTCM/Au electrical switching device; (C) typical I−V characteristics of the Al//PbS/PTCM/Au switching device; (D) pulse switching of the Al//PbS/PTCM/Au device.

segments (Figure 3C) in the nanowire shows that PTCM (the bright part) is amorphous and PbS (the dark part) is single crystal. The HRTEM image (Figure 3D) reveals the exact structure of the PTCM/PbS heterojunction nanowire, indicating the single crystal PbS combined firmly with amorphous PTCM. The HRTEM image of the PbS part exhibits a lattice spacing of 0.34 nm, which is in good agreement with that of the (111) plane of cubic PbS.[43]

As expected, the PTCM/PbS p−n heterojunction nanowire arrays exhibit good diode property. Figure 4A shows the typical I−V curves of PTCM/PbS p−n heterojunction nanowire arrays. The current quickly increases as the increment of applied voltage in the forward bias. For reverse bias, the current transporting through the heterojunction of nanowire arrays is low. The rectification ratio of the diode of PTCM/PbS p−n heterojunction nanowire arrays is up to 15.7 with an applied bias of 1.0 V. An energy level diagram of the PTCM/PbS

heterojunction nanowire array device is shown in Figure S1B (Supporting Information), which shows that the diode nature originates from the interface integration of PTCM and PbS. Under the same measurement condition, the individual PTCM and PbS nanowire arrays only display a semiconductive feature with a conductivity of about 1.08×10^{-6} and 1.22×10^{-6} S/cm, respectively (Figure S5A, Supporting Information).

Interestingly, PTCM/PbS heterojunction nanowire arrays exhibit an excellent electrical switching effect. The working model of the Al/PbS/PTCM/Au electrical switching device was illustrated in Figure 4B. As shown in Figure 4C, when the bias voltage was applied from −2 to +2 V, the PTCM/PbS p−n heterojunction nanowire arrays displayed a significant switching effect from the high resistance state (HRS) to the low resistance state (LRS). At the beginning, the voltage applied on the top Al electrode was positive and increased from zero. During process 1 shown in Figure 4C, the current increased

slowly as the increment of applied voltage. When the applied voltage approached a critical value of about 1.4 V, the current rapidly increased from 1.16 to 152.71 μA (process 2). Then, the current decreased slowly to zero with the decrease of applied voltage (process 3). Upon applying a negative voltage, the current increased quickly with the change of applied voltage in process 4 due to the nanowires being under forward bias. Finally, the applied voltage decreased to zero and the current decreased to zero (process 5). The ON/OFF ratio of PTCM/PbS p−n heterojunction nanowire arrays is about 83.5 at 1.4 V. At the same condition, the ON/OFF ratios of PbS nanowire arrays is about 19 (Figure S5B, Supporting Information), which were far less than the value of PTCM/PbS p−n heterojunction nanowire arrays. The PTCM nanowire arrays do not display electrical switching behavior. At the OFF state, the resistance of PTCM/PbS p−n heterojunction nanowire arrays was far larger than PbS nanowires because the p−n junction was under reverse bias. However, at the ON state, the resistance of PTCM/PbS p−n heterojunction nanowires is higher than that of PbS nanowires. The reason should be due to the fact that only metal Pb bridges provide the resistance in PbS nanowires, while the resistance originated from metal Pb and PTCM in PTCM/PbS p−n heterojunction nanowires. Thus, the ON/OFF ratio of PTCM/PbS p−n heterojunction nanowires is greatly larger than that of PbS nanowires. The electrical switching behavior of PTCM/PbS p−n heterojunction nanowires can be explained as a solid-state electrochemical process.[33] In this process, an internal electric field (E_{in}) at the interface of PbS occurred. When the PTCM/PbS p−n heterojunction nanowire arrays are under reverse bias, the E_{in} is enhanced, which decreases the diffusion of majority carriers. Now, the PTCM/PbS nanowire arrays are at the OFF state of the switch. Meanwhile, the Pb^{2+} ions in PbS are reduced and form Pb filaments toward the top Al electrode. When the metal Pb bridges directly touch both of the top electrodes, the PTCM/PbS p−n heterojunction nanowire arrays are at the ON state of the switch. The device switches off when the applied voltage sweeps back and the metal bridges break from the metal electrodes. The two stable resistance states (HRS and LRS) maintained an initial value under tests of many cycles, as illustrated in Figure 4D, which indicated that the bistable electrical switch of PTCM/PbS p−n heterojunction nanowire arrays is highly stable and repeatable.

CONCLUSION

In summary, we have successfully synthesized the PTCM/PbS p−n axial inserting heterojunction nanowire arrays with a 2.57 μm^2 heterojunction interface. Our results provide new insights into the fabrication of new heterojuction structure materials. The nanowires exhibit excellent rectifying features and diode nature with a rectifying ratio of 15.7. The inorganic/organic p−n heterojunction nanowire arrays show distinct electrical switching properties, and the ON/OFF ratio is up to 83.5. It is significant in material chemistry to create new hetero-junctions on the interface of molecular aggregate structures for realizing synergistic performance.

ASSOCIATED CONTENT

Ⓢ Supporting Information

Cyclic voltammogram of PTCM film; energy level diagram of the PTCM/PbS heterojunction nanowire array device; SEM and TEM images of PTCM and PbS nanowires; energy-dispersive X-microanalysis spectrum (EDS) patterns of the PTCM/PbS heterojunction nanowire; typical I−V curves of PTCM and PbS nanowire arrays; and typical I−V character-istics of the Al/PbS/Au switching device. This material is available free of charge via the Internet at http://pubs.acs.org.

AUTHOR INFORMATION

Corresponding Author
*E-mail: liuhb@iccas.ac.cn (H.L.), ylli@iccas.ac.cn (Y.L.).

Notes
The authors declare no competing financial interest.

ACKNOWLEDGMENTS

REFERENCES

(1) Hochbaum, A. I.; Yang, P. D. *Chem. Rev.* **2010**, *110*, 527.
(2) Liu, H. B.; Xu, J. L.; Li, Y. J.; Li, Y. L. *Acc. Chem. Res.* **2010**, *43*, 11496.
(3) Shen, X. J.; Sun, B. Q.; Liu, D.; Lee, S. T. *J. Am. Chem. Soc.* **2011**, *133*, 19408.
(4) Chen, C. Y.; Retamal, J. R. D.; Lien, D. H.; Chen, M. W.; Wu, I. W.; Ding, Y.; Chueh, Y. L.; Wu, C. I.; He, J. H. *ACS Nano* **2012**, *6*, 9366.
(5) Gudiksen, M. S.; Lauhon, L. J.; Wang, J. F.; Smith, D. C.; Lieber, C. M. *Nature* **2002**, *415*, 617.
(6) Liu, X. F.; Li, Y. L. *Dalton Trans.* **2009**, 6447.
(7) Yang, Y.; Jung, J. H.; Yun, B. K.; Zhang, F.; Pradel, K. C.; Guo, W. Z.; Wang, L. *Adv. Mater.* **2012**, *24*, 5357.
(8) Liu, H. B.; Zhao, Q.; Li, Y. L.; Liu, Y.; Lu, F. S.; Zhuang, J. P.; Wang, S.; Jiang, L.; Zhu, D. B.; Yu, D. P.; Chi, L. F. *J. Am. Chem. Soc.* **2005**, *127*, 1120.
(9) Gan, H. Y.; Liu, H. B.; Li, Y. J.; Zhao, Q.; Li, Y. L.; Wang, S.; Jiu, T. G.; Wang, N.; He, X. R.; Yu, D. P.; Zhu, D. B. *J. Am. Chem. Soc.* **2005**, *127*, 12452.
(10) Zheng, H. Y.; Li, Y. J.; Liu, H. B.; Yin, X. D.; Li, Y. L. *Chem. Soc. Rev.* **2011**, *40*, 4506.
(11) Liu, H. B.; Li, Y. L.; Jiang, L.; Luo, H. Y.; Xiao, S. Q.; Fang, H. J.; Li, H. M.; Zhu, D. B.; Yu, D. P.; Xu, J.; Xiang, B. *J. Am. Chem. Soc.* **2002**, *124*, 13370.
(12) Li, Y. J.; Li, X. F.; Li, Y. L.; Liu, H. B.; Wang, S.; Gan, H. Y.; Li, J. B.; Wang, N.; He, X. R.; Zhu, D. B. *Angew Chem., Int. Ed.* **2006**, *45*, 3639.
(13) Huang, C. S.; Wen, L. P.; Liu, H. B.; Li, Y. L.; Liu, X. F.; Yuan, M. J.; Zhai, J.; Jiang, L.; Zhu, D. B. *Adv. Mater.* **2009**, *17*, 1721.
(14) Huang, C. S.; Li, Y. L.; Song, Y. L.; Li, Y. J.; Liu, H. B.; Zhu, D. B. *Adv. Mater.* **2010**, *22*, 3532.
(15) Sanchez, C.; Belleville, P.; Popall, M.; Nicole, L. *Chem. Soc. Rev.* **2011**, *40*, 696.
(16) Zhang, W. X.; Yang, S. H. *Acc. Chem. Res.* **2009**, *42*, 1617.
(17) Gao, P. X.; Ding, Y.; Mai, W.; Hughes, W. L.; Lao, C. S.; Wang, Z. L. *Science* **2005**, *309*, 1700.
(18) Lu, G.; Farha, O. K.; Hupp, J. T. *Adv. Mater.* **2012**, DOI: 10.1002/adma.201202116.
(19) Yang, Y.; Guo, W. X.; Zhang, Y.; Ding, Y.; Wang, X.; Wang, Z. L. *Nano Lett.* **2011**, *11*, 4812.
(20) Bessire, C. D.; Björk, M. T.; Schmid, H.; Schenk, A.; Reuter, K. B.; Riel, H. *Nano Lett.* **2011**, *11*, 4195.
(21) Nikoobakht, B.; Herzing, A. *ACS Nano* **2010**, *4*, 5877.
(22) Wang, D. A.; Liu, Y.; Wang, C. W.; Zhou, F.; Liu, W. M. *ACS Nano* **2009**, *3*, 1249.
(23) Cui, S.; Li, Y. L.; Guo, Y. B.; Liu, H. B.; Song, Y. L.; Xu, J. L.; Lv, J.; Zhu, M.; Zhu, D. B. *Adv. Mater.* **2008**, *20*, 309.
(24) Yan, R. X.; Liang, W. J.; Fan, R.; Yang, P. D. *Nano Lett.* **2009**, *9*, 3820.

(25) Willinger, M. G.; Neri, G.; Rauwel, E.; Bonavita, A.; Micali, G.; Pinna, N. *Nano Lett.* **2008**, *8*, 4201.

(26) Liu, H. B.; Zuo, Z. C.; Guo, Y. B.; Li, Y. J.; Li, Y. L. *Angew. Chem., Int. Ed.* **2010**, *49*, 2705.

(27) Peng, H. L.; Xie, C.; Schoen, D. T.; Mcllwrath, K.; Zhang, X. F.; Cui, Y. *Nano Lett.* **2007**, *7*, 3734.

(28) Guo, Y. B.; Zhang, Y. J.; Liu, H. B.; Lai, S. W.; Li, Y. L.; Li, Y. J.; Hu, W. P.; Wang, S.; Che, C. M.; Zhu, D. B. *J. Phys. Chem. Lett.* **2010**, *1*, 327.

(29) Kovtyukhova, N. I.; Mallouk, T. E. *Adv. Mater.* **2005**, *17*, 187.

(30) Tong, G. S. M.; Chow, P. K.; Che, C.-M. *Angew. Chem., Int. Ed.* **2010**, *49*, 9206.

(31) Cui, S.; Liu, H. B.; Gan, L. B.; Li, Y. L.; Zhu, D. B. *Adv. Mater.* **2008**, *20*, 2918.

(32) Chen, N.; Qian, X. M.; Lin, H. W.; Liu, H. B.; Li, Y. L. *J. Mater. Chem.* **2012**, *22*, 11068.

(33) Qian, X. M.; Liu, H. B.; Chen, N.; Zhou, H. Q.; Sun, L. F.; Li, Y. J.; Li, Y. L. *Inorg. Chem.* **2012**, *51*, 6771.

(34) Guo, Y. B.; Tang, Q. X.; Liu, H. B.; Zhang, Y. J.; Li, Y. L.; Hu, W. P.; Wang, S.; Zhu, D. B. *J. Am. Chem. Soc.* **2008**, *130*, 9198.

(35) Guo, Y. B.; Liu, H. B.; Li, Y. J.; Li, G. X.; Zhao, Y. J.; Song, Y. L.; Li, Y. L. *J. Phys. Chem. C* **2009**, *113*, 12669.

(36) Liu, H. B.; Cui, S.; Guo, Y. B.; Li, Y. L.; Huang, C. S.; Zuo, Z. C.; Yin, X. D.; Song, Y. L.; Zhu, D. B. *J. Mater. Chem.* **2009**, *19*, 1031.

(37) Briseno, A. L.; Holcombe, T. W.; Boukai, A. I.; Garnett, E. C.; Shelton, S. W.; Fréchet, J. M. J.; Yang, P. D. *Nano Lett.* **2010**, *10*, 334.

(38) Wang, W.; Du, C.; Zhong, D.; Hirtz, M.; Wang, Y.; Lu, N.; Wu, L.; Ebeling, D.; Li, L.; Fuchs, H.; Chi, L. *Adv. Mater.* **2009**, *46*, 4721.

(39) Lin, H. W.; Liu, H. B.; Qian, X. M.; Lai, S. W.; Li, Y. J.; Chen, N.; Ouyang, C. B.; Che, C. M.; Li, Y. L. *Inorg. Chem.* **2011**, *50*, 7749.

(40) Chen, N.; Qian, X. M.; Lin, H. W.; Liu, H. B.; Li, Y. J.; Li, Y. L. *Dalton Trans.* **2011**, *40*, 10804.

(41) Novotny, C. J.; Yu, E. T.; Yu, P. K. L. *Nano Lett.* **2008**, *8*, 775.

(42) Izuhara, D.; Swager, T. M. *J. Am. Chem. Soc.* **2009**, *131*, 17724.

(43) Jang, Y.; Song, Y. M.; Kim, H. S.; Cho, Y. J.; Seo, Y. S.; Jung, G. B.; Lee, C. W.; Park, J.; Jung, M.; Kim, J.; Kim, B.; Kim, J. G.; Kim, Y. J. *ACS Nano* **2010**, *4*, 2391.

6974

dx.doi.org/10.1021/ic400302e | *Inorg. Chem.* 2013, 52, 6969–6974